

## A variable-DOF single-loop 7R spatial mechanism with five motion modes

**Citation for published version:**

Kong, X 2018, 'A variable-DOF single-loop 7R spatial mechanism with five motion modes', *Mechanism and Machine Theory*, vol. 120, pp. 239-249. <https://doi.org/10.1016/j.mechmachtheory.2017.10.005>

**Digital Object Identifier (DOI):**

[10.1016/j.mechmachtheory.2017.10.005](https://doi.org/10.1016/j.mechmachtheory.2017.10.005)

**Link:**

[Link to publication record in Heriot-Watt Research Portal](#)

**Document Version:**

Peer reviewed version

**Published In:**

Mechanism and Machine Theory

**General rights**

Copyright for the publications made accessible via Heriot-Watt Research Portal is retained by the author(s) and / or other copyright owners and it is a condition of accessing these publications that users recognise and abide by the legal requirements associated with these rights.

**Take down policy**

Heriot-Watt University has made every reasonable effort to ensure that the content in Heriot-Watt Research Portal complies with UK legislation. If you believe that the public display of this file breaches copyright please contact [open.access@hw.ac.uk](mailto:open.access@hw.ac.uk) providing details, and we will remove access to the work immediately and investigate your claim.

# A variable-DOF single-loop 7R spatial mechanism with five motion modes

Xianwen Kong

*School of Engineering and Physical Sciences, Heriot-Watt University,  
Edinburgh, UK, EH14 4AS Tel: +44(0)1314513688*

---

## Abstract

This paper is about the construction and reconfiguration analysis of a novel variable-DOF (or kinematotropic) single-loop 7R spatial mechanism, which is composed of seven R (revolute) joints. Firstly, the novel variable-DOF single-loop 7R spatial mechanism is constructed from a general variable-DOF single-loop 7R spatial mechanism and a plane symmetric Bennett joint 6R mechanism for circular translation. The reconfiguration analysis is then carried out in the configuration space by solving a set of kinematic loop equations based on dual quaternions and the natural exponential function substitution using tools from algebraic geometry. The analysis shows that the variable-DOF single-loop 7R spatial mechanism has five motion modes, including a 2-DOF planar 5R mode, two 1-DOF spatial 6R modes, and two 1-DOF spatial 7R modes and can transit between the 2-DOF planar 5R mode and each of the other motion modes through two transition configurations. There are two transition configurations from which the mechanism can switch among its four 1-DOF motion modes.

*Keywords:* Variable-DOF mechanism, reconfiguration analysis, dual quaternions, algebraic geometry, configuration space

---

## 1. Introduction

Variable-DOF (or kinematotropic) mechanisms [1, 2, 3, 4, 5, 6, 7, 8, 9] are a class of reconfigurable mechanisms. Although the variable-DOF mechanisms could be dated back to 1669 [10] when the Wren mechanism was

---

*Email address:* X.Kong@hw.ac.uk (Xianwen Kong)

*Preprint submitted to Mech Mach Theory*

*October 7, 2017*

proposed, such mechanisms were brought to the attention of researchers in 1996 when reference [1] was published. Like in several other areas of mechanism science [11], some earlier variable-DOF mechanisms, such as the variable-DOF mechanism proposed in [12], might have been ignored by many researchers due to the language and discipline constraints.

Several approaches have been proposed for the type synthesis of variable-DOF single-loop mechanisms [2, 7, 8, 9] and parallel mechanisms [3, 5, 6]. A variable-DOF single-loop 7R spatial mechanism with a 1-DOF 6R mode, a 1-DOF spatial 7R mode and a 2-DOF serial 2R mode was presented in [13]. A variable-DOF 6R spatial mechanism with a 1-DOF spatial 6R mode and a 2-DOF serial 2R mode was presented in [14]. The variable-DOF 7R mechanisms proposed so far [7, 9] have up to three 5R, 6R or 7R motion modes.

Meanwhile, several methods have been proposed for the reconfiguration analysis of variable-DOF mechanisms. For example, tools from algebraic geometry [15] have been used for the reconfiguration analysis of single-loop variable-DOF mechanisms [7, 9, 13] and variable-DOF parallel mechanisms [16, 17, 18]. Using these methods, the kinematic equations are formulated by decomposing a mechanism into two (for single-loop mechanisms) or more (for parallel mechanisms) serial kinematic chains and equations describing each operation mode are obtained. The reconfiguration analysis of certain variable-DOF planar Wunderlich mechanisms [19] and single-loop spatial 6R mechanisms [14] has been thoroughly studied. The reconfiguration analysis of a reconfigurable cube mechanism, which is a spatial 8R mechanisms with several 2- or 3-DOF motion modes, has been presented in [21]. In addition, local mobility analysis of variable-DOF mechanisms has been dealt with in [20, 22].<sup>1</sup> The current approaches to the reconfiguration analysis of variable-DOF mechanisms have certain limitations although they have their own merits. For example, the symbolic approach [14] is limited to variable-DOF 6R mechanisms. The method in [21] is only applicable to variable-DOF mechanisms that the joint axes of certain two non-adjacent R joints can become collinear during motion. The approach in [7, 9, 13] suffers from the drawback associated with tangent half-angle substitution since certain joint

---

<sup>1</sup>The variable-DOF mechanism in which several 1-DOF 5R or 6R motion modes are obtained from a 3-DOF 8R mechanism by locking a set of two joints [23] is out of the scope of this paper.

angle is often equal to  $180^\circ$  in a transition configuration of a variable-DOF mechanism. Recently, a method for the reconfiguration analysis of multi-mode single-loop mechanism in the configuration space has been proposed in [24]. A novel multi-mode 1-DOF (degree-of-freedom) 7R spatial mechanism has been found to have three motion modes, including a planar 4R mode, an orthogonal Bricard 6R mode and a plane symmetric 6R mode. Using this approach, a set of kinematic loop equations is derived by using dual quaternions<sup>2</sup> and the natural exponential function substitution and solved using tools from algebraic geometry. Using dual quaternions, a set of kinematic loop equations, which is composed of six polynomial equations, can be formulated effectively. This would provide an efficient approach to the reconfiguration analysis of variable-DOF single-loop mechanisms.

Despite the above advances, the research on variable-DOF spatial mechanisms is still in its infancy. In addition to developing variable-DOF mechanisms for practical applications, some theoretical questions are yet to answer. For example, what is the maximum number of motion modes of variable-DOF mechanisms with the same topological structure, such as variable-DOF single-loop 7R mechanisms?

As a step forward to answer the question “What is the maximum number of motion modes of variable-DOF single-loop 7R mechanisms?”, this paper will investigate the construction and reconfiguration analysis of a novel variable-DOF 7R spatial mechanism that has more motion modes than the ones in the literature. This spatial 7R mechanism is a special case of the variable-DOF 7R spatial mechanism proposed in [7], which may have a 2-DOF planar 5R mode and one or two 1-DOF spatial 7R mode. As will be shown later, the 7R variable-DOF mechanism has five motion modes, including a 2-DOF planar 5R mode, two 1-DOF spatial 6R modes and two 1-DOF spatial 7R modes.

This paper is organized as follows. In Section 2, the kinematic loop equations based on dual quaternions and the natural exponential function substitution [24] are recalled to facilitate the understanding of this paper. The construction of a novel variable-DOF spatial 7R mechanism is given in Section 3. The motion modes and transition configurations of the novel

---

<sup>2</sup>Different variations and notations of dual quaternions were used in [25, 26, 27, 28, 29, 30, 31, 32]. For other mathematical tools in kinematics, please refer to [30, 31, 33, 34, 35] and the references therein.

variable-DOF 7R single-loop spatial mechanism are identified in Sections 4 and 5 respectively. Finally, conclusions are drawn.

## 2. Kinematic loop equations based on dual quaternions and the natural exponential function substitution

In this section, the procedure for formulating the kinematic loop equations based on dual quaternions and the natural exponential function substitution [24] is recalled to facilitate the understanding of this paper. Throughout this paper, the link parameters of mechanisms are represented by D-H (Denavit-Hartenberg) parameters  $d_i$ ,  $\theta_i$ ,  $L_i$  and  $\alpha_i$ .  $S(*)$  and  $C(*)$  represent  $\sin(*)$  and  $\cos(*)$  respectively.

Let  $I$  be the imaginary unit and  $u_i = e^{I\theta_i}$ . The dual quaternions corresponding to no motion, translation along  $X_i$ -axis by  $L_i$ , translation along  $Z_i$ -axis by  $d_i$ , rotation about  $X_i$ -axis by  $\alpha_i$ , rotation about  $Z_i$ -axis by  $\theta_i$  are

$$\begin{aligned} Q_E &= 1 \\ Q_{TranX_i} &= 1 + \epsilon(L_i/2)\mathbf{i} \\ Q_{TranZ_i} &= 1 + \epsilon(d_i/2)\mathbf{k} \\ Q_{RotX_i} &= C(\alpha_i/2) + S(\alpha_i/2)\mathbf{i} \\ \tilde{Q}_{RotZ_i} &= \begin{cases} (1 + u_i) + (1 - u_i)I\mathbf{k} & \text{if joint } i \text{ is an R (revolute) joint} \\ C(\theta_i/2) + S(\theta_i/2)\mathbf{k} & \text{if joint } i \text{ is a P (prismatic) joint} \end{cases} \end{aligned}$$

The product of dual quaternions satisfies the following rules:

$$\begin{aligned} \epsilon &\neq 0 \\ \epsilon^2 &= 0 \\ \mathbf{i}^2 &= \mathbf{j}^2 = \mathbf{k}^2 = \mathbf{ijk} = -1 \\ \mathbf{ij} &= \mathbf{k} = -\mathbf{ji} \\ \mathbf{jk} &= \mathbf{i} = -\mathbf{kj} \\ \mathbf{ki} &= \mathbf{j} = -\mathbf{ik} \end{aligned}$$

In a single-loop mechanism composed of  $n$  R joints numbered from 1 to  $n$  in sequence, the  $n$  links of the mechanism are also numbered from 1 to  $n$  with joints  $i$  and  $(i+1)$  located on link  $i$  ( $1, 2, \dots, n$ ). For brevity and clarity, the frame (link  $n$ ) is highlighted, and the link numbers are not shown in the figures throughout this paper. The set of kinematic loop equations that has no extraneous solution can be obtained for this single-loop mechanism using the following three steps.

Step 1 Derive a set of kinematic loop equations in dual quaternions by using the natural exponential function substitution.

The set of kinematic loop equations of a loop composed of  $n$  R joints can be represented as [24]

$$\prod_{i=1}^n (\tilde{Q}_{RotZ_i} Q_{TranZ_i} Q_{TranX_i} Q_{RotX_i}) = [2^n (\prod_{i=1}^n u_i)^{1/2}] Q_E \quad (1)$$

Step 2 Formulate a set of six polynomial equations.

Taking the second, third, fourth, sixth, seventh and eighth scalar equations of Eq. (1), we obtain a set of 6 equations in  $u_i$  ( $i = 1, 2, \dots, n$ ) as

$$\begin{cases} e_1(u_1, u_2, \dots, u_n) = 0 \\ e_2(u_1, u_2, \dots, u_n) = 0 \\ e_3(u_1, u_2, \dots, u_n) = 0 \\ g_1(u_1, u_2, \dots, u_n) = 0 \\ g_2(u_1, u_2, \dots, u_n) = 0 \\ g_3(u_1, u_2, \dots, u_n) = 0 \end{cases} \quad (2)$$

All the solutions to Eq. (2) in which at least one joint variable satisfies Eq.(3) are extraneous since there is no real solution of  $\theta_i$  to Eq.(3).

$$u_i = 0 \quad (3)$$

Step 3 Obtain a set of polynomial equations without extraneous solutions.

One can first add an equation  $u_1 u_2 \dots u_n v - 1 = 0$  with an extra variable  $v$  to Eq. (2) and then compute an elimination ideal that eliminates  $v$  using the Maple command *EliminationIdeal* to obtain a new set of equations with the extraneous solutions excluded [24, 29].

### 3. Constructions of a novel variable-DOF 7R spatial mechanism

Using the construction approach [36], a single-DOF multi-mode single-loop mechanism can be constructed from two single-loop mechanisms by first

letting these two single-DOF compositional mechanisms have certain number of common joints and then construct multi-mode single-loop mechanisms which are each composed of the common joints and all the remaining joints of the compositional mechanisms. In this section, a novel variable-DOF 7R spatial mechanism will be constructed using this approach.

Figure 1a shows a variable-DOF single-loop spatial 7R mechanism 1-2-3-4-5-6-7-1, which is obtained by inserting two R joints to a 2-DOF planar 5R mechanism, usually has one 2-DOF planar 5R mode and one or two 1-DOF spatial 7R modes [7]. This 7R mechanism meets the following conditions:

$$\alpha_1 = -\alpha_2, \alpha_5 = -\alpha_6 \text{ and } \alpha_3 = \alpha_4 = \alpha_7 = 0.$$

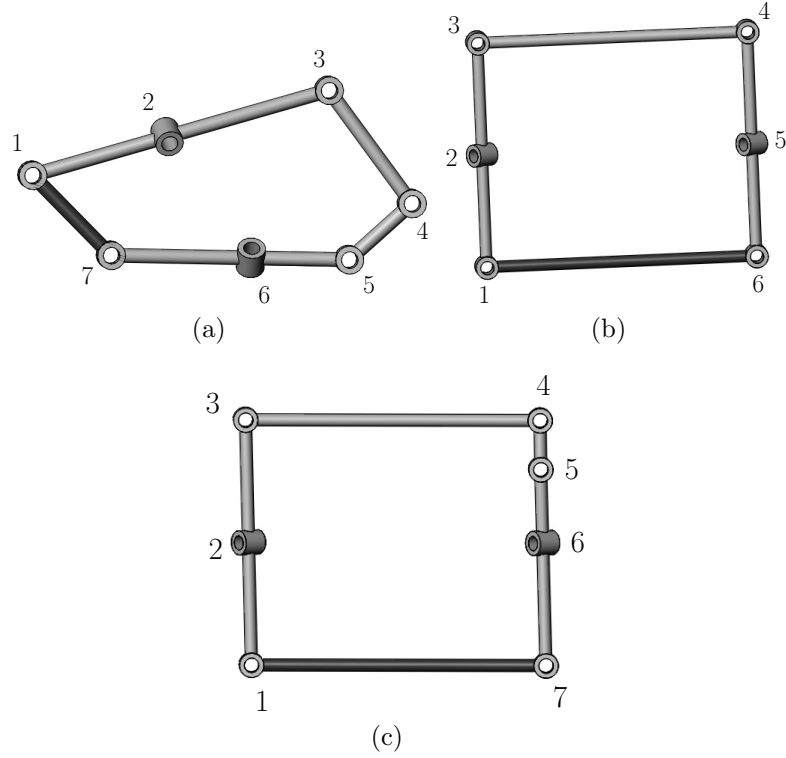


Figure 1: Construction of a novel variable-DOF single-loop spatial 7R mechanism: (a) A general variable-DOF spatial 7R mechanism in planar 5R mode, (b) A plane symmetric Bennett joint 6R mechanism for circular translation in a transition configuration, and (c) A novel variable-DOF spatial 7R mechanism in a transition configuration.

Figure 1b shows a single-loop plane symmetric Bennett joint 6R mechanism for circular translation 1-2-3-4-5-6-1, which meets the conditions com-

mon to the 6R mechanisms for circular translation [37], Bennett joint 6R [38] and plane symmetric 6R mechanism. This 6R mechanism meets the following conditions:

$d_i = 0, i = 1, 2, \dots, 6, L_1 = L_2 = L_4 = L_5, L_3 = L_6, \alpha_3 = \alpha_6 = 0$  and  $\alpha_1 = \alpha_5 = -\alpha_2 = -\alpha_4$ .

Using the constructions approach [36], we can obtain a new variable-DOF single-loop spatial 7R mechanism 1-2-3-4-5-6-7-1 (Fig. 1c) by letting the 7R mechanism in Fig. 1a and the 6R mechanism in Fig. 1b have six common joints. Specifically, let the joint axes of joints 1, 2, 3, 4, 6, 7 in the 7R mechanism in Fig. 1a coincide with the joint axes of joints 1, 2, 3, 4, 5, 6 in the 6R mechanism in Fig. 1b and number these joints as 1, 2, 3, 4, 6 and 7. Joint 5 in new 7R mechanism is joint 5 of the 7R mechanism in Fig. 1a. One can obtain that this new 7R mechanism meets the following conditions:

$d_i = 0, i = 1, 2, \dots, 7, \alpha_1 = -\alpha_2 = -\alpha_5 = \alpha_6, L_1 = L_2 = L_6 = L_4 + L_5, L_3 = L_7$  and  $\alpha_3 = \alpha_4 = \alpha_7 = 0$ .

Please note the above conditions on  $d_5, d_6, L_4$  and  $L_5$  are not general since we focus on the case that the 7R mechanism can reach a configuration in which all the links form a rectangle.

#### 4. Motion mode analysis

In this section, we will deal with the motion mode analysis of the variable-DOF 7R spatial mechanism in joint space by obtaining a set of loop equations following the procedure in Section 2 and solving the set of equations using tools from algebraic geometry.

A variable-DOF 7R spatial mechanism with the following link parameters will be used as an example.

$$\begin{aligned} d_i &= 0, i = 1, 2, \dots, 7 \\ L_1 &= L_2 = L_6 = 5, L_4 = 2, L_5 = 3, L_3 = L_7 = 12 \\ \alpha_1 &= \alpha_6 = 2\text{atan}(2) \\ \alpha_2 &= \alpha_5 = -2\text{atan}(2) \\ \alpha_3 &= \alpha_4 = \alpha_7 = 0 \end{aligned}$$

Substituting the link parameters of the variable-DOF 7R mechanism into Eq. (1), we have

$$\prod_{i=1}^7 (\tilde{Q}_{RotZ_i} Q_{TranZ_i} Q_{TranX_i} Q_{RotX_i}) = 128(u_1 u_2 u_3 u_4 u_5 u_6 u_7)^{1/2} Q_E \quad (4)$$



Taking the second, third, fourth, sixth, seventh and eighth scalar equations of Eq. (4) and simplifying these equations by dividing them with certain constants, we obtain the following set of kinematic loop equations.

$$\begin{cases} e_1(u_1, u_2, \dots, u_7) = 0 \\ e_2(u_1, u_2, \dots, u_7) = 0 \\ e_3(u_1, u_2, \dots, u_7) = 0 \\ g_1(u_1, u_2, \dots, u_7) = 0 \\ g_2(u_1, u_2, \dots, u_7) = 0 \\ g_3(u_1, u_2, \dots, u_7) = 0 \end{cases} \quad (5)$$

where

$$e_1 = u_1 u_2 u_3 u_4 u_5 u_6 + u_2 u_3 u_4 u_5 u_6 u_7 - u_1 u_2 u_3 u_4 u_5 + 4u_1 u_3 u_4 u_5 u_6 + 4u_2 u_3 u_4 u_5 u_7 - u_3 u_4 u_5 u_6 u_7 - 4u_1 u_3 u_4 u_5 - 4u_3 u_4 u_5 u_7 - 4u_1 u_2 u_6 - 4u_2 u_6 u_7 - u_1 u_2 + 4u_1 u_6 + 4u_2 u_7 - u_6 u_7 + u_1 + u_7,$$

...

$$g_3 = u_1 u_2 u_3 u_4 u_5 u_6 u_7 + 6u_1 u_2 u_3 u_4 u_5 u_6 - u_1 u_2 u_3 u_4 u_5 u_7 - u_1 u_2 u_3 u_4 u_6 u_7 - 6u_1 u_2 u_4 u_5 u_6 u_7 + 4u_1 u_3 u_4 u_5 u_6 u_7 - 6u_2 u_3 u_4 u_5 u_6 u_7 - 6u_1 u_2 u_3 u_4 u_5 + u_1 u_2 u_3 u_4 u_7 - 6u_1 u_2 u_3 u_6 u_7 - 24u_1 u_2 u_4 u_5 u_7 - u_1 u_2 u_5 u_6 u_7 + 24u_1 u_3 u_4 u_5 u_6 - 4u_1 u_3 u_4 u_5 u_7 - 4u_1 u_3 u_4 u_6 u_7 + 6u_1 u_4 u_5 u_6 u_7 - 21u_2 u_3 u_4 u_5 u_6 - 24u_2 u_3 u_4 u_5 u_7 + 6u_3 u_4 u_5 u_6 u_7 + 6u_1 u_2 u_3 u_7 - 4u_1 u_2 u_5 u_7 - 24u_1 u_2 u_6 u_7 - 24u_1 u_3 u_4 u_5 + 4u_1 u_3 u_4 u_7 - 24u_1 u_3 u_6 u_7 + 24u_1 u_4 u_5 u_7 + u_1 u_5 u_6 u_7 + u_2 u_3 u_4 u_5 - 4u_2 u_3 u_4 u_6 - 24u_2 u_4 u_5 u_6 - 4u_3 u_4 u_5 u_6 + 24u_3 u_4 u_5 u_7 - 24u_1 u_2 u_6 + 4u_1 u_2 u_7 + 24u_1 u_3 u_7 + 4u_1 u_5 u_7 - u_1 u_6 u_7 - u_2 u_3 u_4 - 24u_2 u_3 u_6 + 24u_2 u_4 u_5 - 4u_2 u_5 u_6 + 24u_2 u_6 u_7 + 24u_3 u_4 u_5 + 4u_3 u_4 u_6 - 6u_4 u_5 u_6 - 6u_1 u_2 + 24u_1 u_6 + 21u_1 u_7 - 6u_2 u_3 + 4u_2 u_5 + 4u_2 u_6 - 24u_2 u_7 + u_3 u_4 + 24u_3 u_6 + 6u_4 u_5 - u_5 u_6 + 6u_6 u_7 + 6u_1 - 4u_2 + 6u_3 + u_5 + u_6 - 6u_7 - 1.$$

After removing the extraneous solutions from Eq. (5) using Maple command *EliminationIdeal*, we have

$$h_i(u_1, u_2, \dots, u_7) = 0 \quad i = 1, 2, \dots, 60 \quad (6)$$

where

$$h_1 = -u_2^2 u_6 + u_2 u_6^2 + u_2 - u_6,$$

$$h_2 = 6u_2 u_4 u_5 + u_2 u_5 - 6u_2 u_7 - 6u_4 u_5 - u_2 - u_5 + 6u_7 + 1,$$

...

Let  $\mathcal{J} = \langle h_1, h_2, \dots, h_{60} \rangle$  denote the ideal composed of the 60 polynomials associated with Eq. (6). Calculating the prime decomposition of  $\mathcal{J}$  using

computer algebra systems such as Maple, Singular or Magma, we have

$$\mathcal{J} = \bigcap_{j=1}^5 \mathcal{J}_j \quad (7)$$

where the irreducible components,  $\mathcal{J}_j$ , of  $\mathcal{J}$  are<sup>3</sup>:

$$\begin{aligned} \mathcal{J}_1 = < u_2 - 1, u_6 - 1, -3u_1u_3u_4 + 10u_3u_4u_5 - 18u_1u_3 + 12u_4u_5 - 15u_1 + \\ 2u_5 - 10, -6u_1u_3u_4 + 24u_1u_3u_7 + 20u_1u_7 - 5u_3u_4 - 6u_4 + 24u_7 + 15, 18u_1^2u_3^2u_5 + \\ 15u_1^2u_3u_5 + 15u_1u_3^2u_5 - 2u_1u_3u_5^2 + 40u_1u_3u_5 - 2u_1u_3 + 15u_1u_5 + 15u_3u_5 + \\ 18u_5, 5u_3^2u_4^2u_7 + 30u_3^2u_4u_7 + 6u_3u_4^2u_7 - 24u_3u_4u_7^2 + 10u_3u_4u_7 - 24u_3u_4 + 6u_3u_7 + \\ 30u_4u_7 + 5u_7, -18u_1^2u_3u_5 + 12u_1u_4u_5^2 - 15u_1^2u_5 - 15u_1u_3u_5 + 3u_1u_4u_5 + 2u_1u_5^2 - \\ 22u_1u_5 + 2u_1 - 15u_5, 6u_1^2u_3u_4 + 36u_1^2u_3 + 5u_1u_3u_4 - 24u_1u_4u_5 + 30u_1^2 + 30u_1u_3 - \\ 4u_1u_5 + 45u_1 + 30, 20u_1u_4u_7^2 - 5u_3u_4^2u_7 + 30u_1u_4u_7 - 30u_3u_4u_7 - 6u_4^2u_7 + 24u_4u_7^2 + \\ 15u_4u_7 + 24u_4 - 6u_7, 6u_1u_3u_4^2 + 36u_1u_3u_4 - 20u_1u_4u_7 + 5u_3u_4^2 + 30u_3u_4 + 6u_4^2 - \\ 24u_4u_7 + 21u_4 + 6, -18u_1u_3^2u_5 + 3u_3u_5^2u_7 - 15u_1u_3u_5 - 15u_3^2u_5 + 2u_3u_5^2 + \\ 12u_3u_5u_7 - 22u_3u_5 + 2u_3 - 15u_5, -10u_1^2u_4u_7 + 12u_1u_4^2u_5 - 15u_1^2u_4 + 3u_1u_4^2 + \\ 2u_1u_4u_5 - 12u_1u_4u_7 - 12u_1u_4 + 3u_1 - 15u_4, -5u_3^2u_4u_7 + 6u_3u_5u_7^2 - 30u_3^2u_7 - \\ 6u_3u_4u_7 + 4u_3u_5u_7 + 24u_3u_7^2 - 9u_3u_7 + 24u_3 - 30u_7, -6u_1u_3u_4 + 36u_4u_5u_7 - \\ 36u_1u_3 - 5u_3u_4 + 24u_4u_5 + 6u_5u_7 - 30u_1 - 30u_3 + 4u_5 + 24u_7 - 9, -6u_1u_3u_4 + \\ 5u_1u_5u_7 - 36u_1u_3 + 20u_1u_7 - 5u_3u_4 + 6u_5u_7 - 30u_3 - 6u_4 + 4u_5 + 24u_7 - \\ 20, 6u_1u_3^2u_4 + 36u_1u_3^2 + 5u_3^2u_4 - 6u_3u_5u_7 + 30u_1u_3 + 30u_3^2 + 6u_3u_4 - 4u_3u_5 - \\ 24u_3u_7 + 45u_3 + 30 > \end{aligned}$$

$$\mathcal{J}_2 = < -1 + u_5, u_3 - u_1, -u_4 + u_7, u_1u_4 + 1, u_2u_6 - 1, 4u_2u_4^2 + u_4^2 + u_2 + 4, u_4^2u_6 + 4u_4^2 + 4u_6 + 1, u_1u_2 - 4u_2u_4 + 4u_1 - u_4, 4u_1u_6 - u_4u_6 + u_1 - 4u_4 >$$

$$\mathcal{J}_3 = < -1 + u_5, -u_2 + u_6, u_3 - u_1, -u_4 + u_7, 5u_1u_4 + 6u_1 + 6u_4 + 5, 6u_2u_4^2 + 25u_2u_4 + 24u_4^2 + 24u_2 + 25u_4 + 6, 6u_1u_2 + 6u_2u_4 + 24u_1 + 25u_2 + 24u_4 + 25 >$$

$$\begin{aligned} \mathcal{J}_4 = < u_4 + u_1, u_2u_6 - 1, u_4u_7 - 1, u_3u_5 + u_7, u_2u_4^2 + 4u_4^2 + 4u_2 + 1, u_3u_4 + \\ 6u_3 + 6u_4 + 1, 6u_3u_7 + u_3 + u_7 + 6, 4u_4^2u_6 + u_4^2 + u_6 + 4, u_5u_7 - 6u_7^2 + 6u_5 - u_7, u_2u_4 + \\ 4u_2u_7 + 4u_4 + u_7, 6u_4u_5 + u_5 - 6u_7 - 1, 4u_4u_6 + u_6u_7 + u_4 + 4u_7, 8u_2u_3 + 7u_2u_4 + \\ 6u_2 + 29u_3 + 28u_4 + 6, 29u_3u_6 + 28u_4u_6 + 8u_3 + 7u_4 + 6u_6 + 6, 3u_2u_4 + 58u_2u_5 + \\ 14u_2 + 12u_4 + 16u_5 - 9u_7 + 56, 24u_4u_6 + 8u_5u_6 + 6u_4 + 29u_5 + 28u_6 + 18u_7 + 7 > \end{aligned}$$

$$\mathcal{J}_5 = < -u_2 + u_6, u_4u_7 - 1, 6u_1u_4 + 5u_1 + 5u_4 + 6, 5u_1u_7 + 6u_1 + 6u_7 + 5, u_5u_7 - 6u_7^2 + 6u_5 - u_7, u_1u_2 - 4u_2u_4 + 4u_1 - u_4, 6u_4u_5 + u_5 - 6u_7 - 1, 120u_1u_5 - 186u_1 + 155u_5 - 66u_7 - 155, 5u_3u_4 - 24u_1 + 30u_3 + 6u_7 + 5, 25u_3u_5 + 30u_7^2 - 36u_1 -$$

---

<sup>3</sup>These five irreducible components were obtained using the Maple command PrimeDecomposition and verified using Singular and Magma. However, this Maple command led to 15 extraneous irreducible components, which were further removed.

$$11u_7 - 30, 24u_2u_4^2 + 25u_2u_4 + 6u_4^2 + 6u_2 + 25u_4 + 24, 150u_3u_7 + 30u_7^2 + 144u_1 + 25u_3 + 169u_7 + 120, -720u_1^2 + 775u_1u_3 - 666u_1 + 600u_3 - 66u_7 - 55, 24u_2u_4 + 6u_2u_7 + 25u_2 + 6u_4 + 24u_7 + 25, -32u_2u_4 + u_2u_5 - 24u_2 - 8u_4 + 8u_5 - 24u_7 - 31, 360u_2u_3 - 1680u_2u_4 + 1296u_1 - 310u_2 + 45u_3 - 420u_4 - 279u_7 - 310 >$$

The Hilbert dimension of  $\mathcal{J}_1$  is 2 while  $\mathcal{J}_i$  ( $i=2, 3, 4$  and  $5$ ) are all of dimension 1. Then, we obtain five sets of positive-dimension solutions. In the following, we will reveal the motion modes associated with these positive-dimension solutions.

The 2-dimensional vanishing set  $\mathcal{V}(\mathcal{J}_1)$  of  $\mathcal{J}_1$  leads to<sup>4</sup>

$$\begin{cases} u_2 - 1 = 0 \\ u_6 - 1 = 0 \\ \dots \end{cases} \quad (8)$$

i.e.,

$$\begin{cases} \theta_2 = 0 \\ \theta_6 = 0 \\ \dots \end{cases} \quad (9)$$

Equation (9) shows that the motion mode associated with  $\mathcal{V}(\mathcal{J}_1)$  is a 2-DOF planar 5R mode (Fig. 2a). In this motion mode, joints 2 and 6 lose their DOF and the joint axes of joints 1, 3, 4, 5 and 7 are parallel.

The 1-dimensional vanishing set of  $\mathcal{V}(\mathcal{J}_2)$  of  $\mathcal{J}_2$  leads to

$$\begin{cases} -1 + u_5 = 0 \\ u_3 - u_1 = 0 \\ -u_4 + u_7 = 0 \\ u_1u_4 + 1 = 0 \\ u_2u_6 - 1 = 0 \\ \dots \end{cases} \quad (10)$$

---

<sup>4</sup>Here and throughout this paper, only the minimal set of equations that can indicate the characteristics of a motion mode is given, while the remaining equations of the motion mode are omitted for brevity.

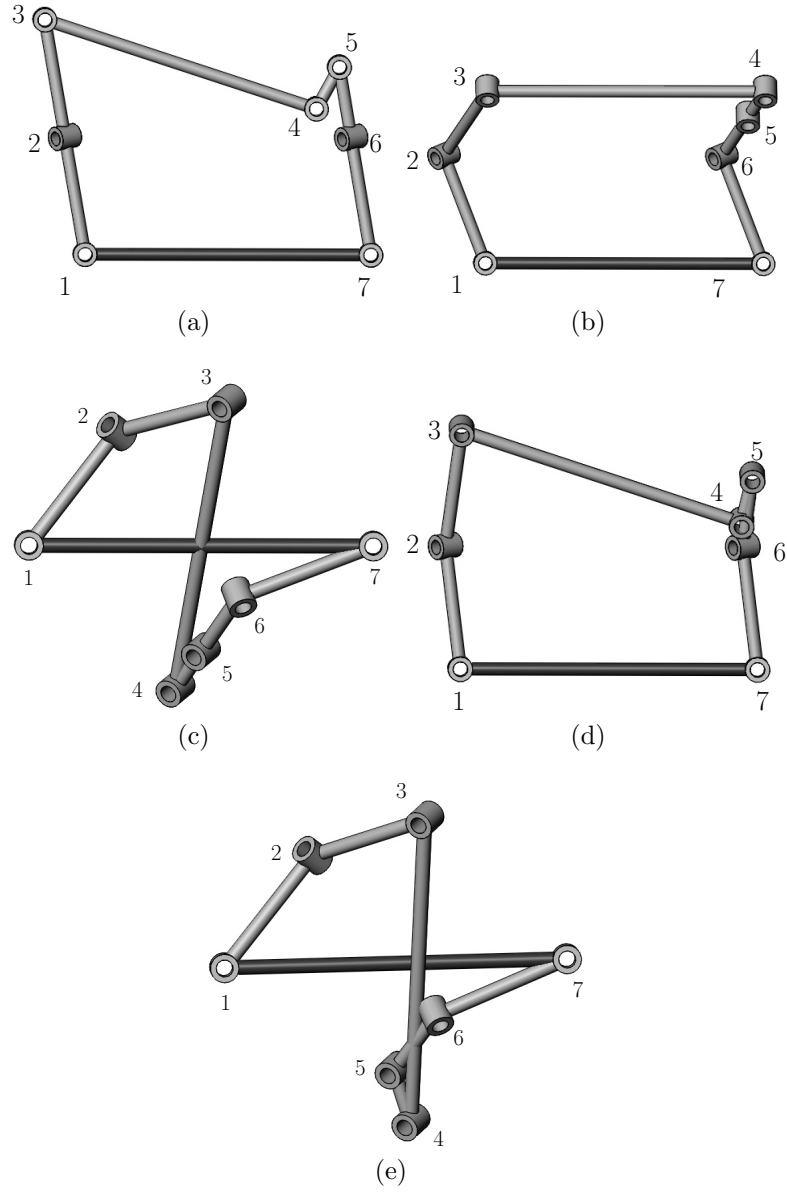


Figure 2: Motion modes of the variable-DOF 7R mechanism: (a) Motion mode 1 (2-DOF planar 5R mode), (b) Motion mode 2 (Circular translational 6R mode), (c) Motion mode 3 (Bennett-joint 6R mode), (d) Motion mode 4 (Quasi-circular-translational 7R mode), and (e) Motion mode 5 (Quasi-Bennett-joint 7R mode).

i.e.,

$$\begin{cases} \theta_5 = 0 \\ \theta_1 = \theta_3 \\ \theta_4 = \theta_7 \\ \theta_4 = 180^\circ - \theta_1 \\ \theta_6 = -\theta_2 \\ \dots \end{cases} \quad (11)$$

Equation (11) shows that the motion mode associated with  $\mathcal{V}(\mathcal{J}_2)$  is a 1-DOF circular translational 6R mode (Fig. 2b). In this motion mode, joint 5 loses its DOF.

Table 1: Five motion modes of the variable-DOF 7R mechanism.

No	DOF	Type	Constraint equations	Description
1	2-DOF	5R	$\begin{cases} \theta_2 = 0 \\ \theta_6 = 0 \\ \dots \end{cases}$	Planar 5R mode (Fig. 2a): The axes of joints 1, 3, 4, 5 and 7 are parallel, and joints 2 and 6 lose their DOF.
2	1-DOF	6R	$\begin{cases} \theta_5 = 0 \\ \theta_1 = \theta_3 \\ \theta_4 = \theta_7 \\ \theta_4 = 180^\circ - \theta_1 \\ \theta_6 = -\theta_2 \\ \dots \end{cases}$	Circular translational 6R mode (Fig. 2b): joints 5 loses its DOF. Link 1 (2) undergoes circular translation with respect to link 6 (4).
3			$\begin{cases} \theta_5 = 0 \\ \theta_2 = \theta_6 \\ \theta_1 = \theta_3 \\ \theta_4 = \theta_7 \\ \dots \end{cases}$	Bennett-joint 6R mode (Fig. 2c): joints 5 loses its DOF.
4		7R	$\begin{cases} \theta_4 = \theta_1 + 180^\circ \\ \theta_6 = -\theta_2 \\ \theta_7 = -\theta_4 \\ \dots \end{cases}$	Quasi-circular-translational 7R mode (Fig. 2d): In this motion mode, the configurations of the mechanisms are close to those of the circular-translation 6R mode.
5			$\begin{cases} \theta_6 = \theta_2 \\ \theta_7 = -\theta_4 \\ \dots \end{cases}$	Quasi-Bennett-joint 7R mode (Fig. 2e): In this motion mode, the configurations of the mechanism are close to those of the Bennett-joint 6R mode.

Similarly, one can identify one motion mode associated with the vanishing set of each of the remaining irreducible components.

In summary, all the five motion modes of the variable-DOF 7R mechanism,

including a 2-DOF planar 5R mode, two 1-DOF 6R modes, and two 1-DOF 7R modes, have been obtained and are given in Table 1.

## 5. Transition configuration analysis

For the five motion modes of the variable-DOF 7R mechanism obtained in Section 4, the transition configurations between each pair of motion modes of the variable-DOF 7R mechanism will be identified. The transition configurations between two motion modes are configurations common to both the motion modes. Solving the set of the equations composed of both sets of equations associated with these motion modes, one can obtain the transition configurations.

Solving the equations associated with the motion mode 1 (planar 5R mode) [see Eq. (8) or (9)] and motion mode 2 (circular-translational 6R mode) [see Eq. (10) or (11)] of the variable-DOF 7R mechanism, we have

$$\left\{ \begin{array}{l} \theta_2 = 0 \\ \theta_5 = 0 \\ \theta_6 = 0 \\ \theta_1 = \theta_3 \\ \theta_4 = \theta_7 \\ \theta_4 = 180^\circ - \theta_1 \\ \dots \end{array} \right. \quad (12)$$

Solving Eq. (12), we obtain the two transition configurations,  $T(1 \wedge 2)$ , between motion mode 1 and motion mode 2.

$$\left\{ \begin{array}{l} \theta_1 = 90^\circ \\ \theta_2 = 0 \\ \theta_3 = 90^\circ \\ \theta_4 = 90^\circ \\ \theta_5 = 0 \\ \theta_6 = 0 \\ \theta_7 = 90^\circ \end{array} \right. \quad (13)$$

$$\left\{ \begin{array}{l} \theta_1 = -90^\circ \\ \theta_2 = 0 \\ \theta_3 = -90^\circ \\ \theta_4 = -90^\circ \\ \theta_5 = 0 \\ \theta_6 = 0 \\ \theta_7 = -90^\circ \end{array} \right. \quad (14)$$

All the transition configurations of the 7R mechanism have been obtained and listed in Table 2.

Table 2: Transition configurations,  $T(i \wedge j)$ , between operation mode  $i$  and operation mode  $j$ .

Case	No	Constraint equations	Description
$T(1 \wedge 2)$	T1	$\begin{cases} \theta_1 = -90^\circ \\ \theta_2 = 0 \\ \theta_3 = -90^\circ \\ \theta_4 = -90^\circ \\ \theta_5 = 0 \\ \theta_6 = 0 \\ \theta_7 = -90^\circ \end{cases}$	
	T2	$\begin{cases} \theta_1 = 90^\circ \\ \theta_2 = 0 \\ \theta_3 = 90^\circ \\ \theta_4 = 90^\circ \\ \theta_5 = 0 \\ \theta_6 = 0 \\ \theta_7 = 90^\circ \end{cases}$	
$T(1 \wedge 3)$	T3	$\begin{cases} \theta_1 = -146.4427^\circ \\ \theta_2 = 0 \\ \theta_3 = -146.4427^\circ \\ \theta_4 = 146.4427^\circ \\ \theta_5 = 0 \\ \theta_6 = 0 \\ \theta_7 = 146.4427^\circ \end{cases}$	
	T4	$\begin{cases} \theta_1 = 146.4427^\circ \\ \theta_2 = 0 \\ \theta_3 = 146.4427^\circ \\ \theta_4 = -146.4427^\circ \\ \theta_5 = 0 \\ \theta_6 = 0 \\ \theta_7 = -146.4427^\circ \end{cases}$	



Continued on next page

**Table 2 – continued from previous page**

Case	No	Constraint equations	Description
$T(1 \wedge 4)$	T5	$\left\{ \begin{array}{l} \theta_1 = -90^\circ \\ \theta_2 = 0 \\ \theta_3 = -108.9246^\circ \\ \theta_4 = 90^\circ \\ \theta_5 = -161.0754^\circ \\ \theta_6 = 0 \\ \theta_7 = -90^\circ \end{array} \right.$	
		$\left\{ \begin{array}{l} \theta_1 = 90^\circ \\ \theta_2 = 0 \\ \theta_3 = 108.9246^\circ \\ \theta_4 = -90^\circ \\ \theta_5 = 161.0754^\circ \\ \theta_6 = 0 \\ \theta_7 = 90^\circ \end{array} \right.$	
$T(1 \wedge 5)$	T7	$\left\{ \begin{array}{l} \theta_1 = -146.4427^\circ \\ \theta_2 = 0 \\ \theta_3 = -134.2292^\circ \\ \theta_4 = -146.4427^\circ \\ \theta_5 = -79.3281^\circ \\ \theta_6 = 0 \\ \theta_7 = 146.4427^\circ \end{array} \right.$	
		$\left\{ \begin{array}{l} \theta_1 = 146.4427^\circ \\ \theta_2 = 0 \\ \theta_3 = 134.2292^\circ \\ \theta_4 = 146.4427^\circ \\ \theta_5 = 79.3281^\circ \\ \theta_6 = 0 \\ \theta_7 = -146.4427^\circ \end{array} \right.$	
Continued on next page			



**Table 2 – continued from previous page**

Case	No	Constraint equations	Description
Other cases	T9	$\left\{ \begin{array}{l} \theta_1 = 180^\circ \\ \theta_2 = 180^\circ \\ \theta_3 = 180^\circ \\ \theta_4 = 0 \\ \theta_5 = 0 \\ \theta_6 = 180^\circ \\ \theta_7 = 0 \end{array} \right.$	
	T10	$\left\{ \begin{array}{l} \theta_1 = 0 \\ \theta_2 = 180^\circ \\ \theta_3 = 0 \\ \theta_4 = 180^\circ \\ \theta_5 = 0 \\ \theta_6 = 180^\circ \\ \theta_7 = 180^\circ \end{array} \right.$	

From Table 2, one can conclude that the variable-DOF 7R mechanism can switch among its motion modes in theory as shown in Fig. 3. The mechanism can transit between the 2-DOF planar 5R mode and each of the other modes through two transition configurations. There are two transition configurations from which the mechanism can switch among its four 1-DOF modes.

Using the well-documented approach based on screw theory (see for example [7, 39]), it can be readily proved that in each transition configuration, the variable-DOF 7R mechanism has generally three instantaneous DOF.

## 6. Conclusions

A construction method has been proposed for obtaining variable-DOF 7R mechanisms with more motion modes than an existing variable-DOF 7R mechanism. The reconfiguration analysis of a novel variable-DOF 7R spatial mechanism has shown that the 7R mechanism has five motion modes, including a 2-DOF planar 5R mode, two 1-DOF 6R modes, and two 1-DOF 7R modes and can transit between the 2-DOF 5R mode and each of the other modes through two transition configurations. There are two transition configurations from which the mechanism can switch among its four 1-DOF modes. The method based on dual quaternions and the natural exponential function substitution [24] has been found to be effi-

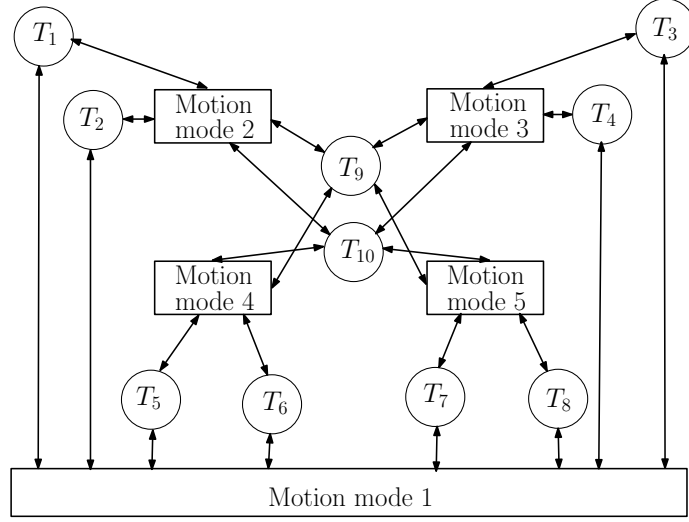


Figure 3: Reconfiguration of the variable-DOF 7R mechanism among its five motion modes through ten transition configurations.

cient for the reconfiguration analysis of variable-DOF 7R spatial mechanisms in the configuration space.

The work is being extended to the construction and reconfiguration analysis of other variable-DOF single-loop and multi-loop mechanisms, such as 7R variable-DOF mechanism that has more than five motion modes, and the development of foldable parallel manipulators.

## Acknowledgment

The author would like to thank the Engineering and Physical Sciences Research Council (EPSRC), United Kingdom, for the support under grant No. EP/K018345/1.

## References

- [1] Wohlhart, K., 1996, “Kinematotropic linkages,” *Recent Advances in Robot Kinematics*, J. Lenarcic and V. Parenti-Castelli (Eds). Kluwer Academic, Dordrecht, The Netherlands, pp. 359–368.
- [2] Galletti, C. and Fanghella, P., 2001, “Single-loop kinematotropic mechanisms,” *Mechanism and Machine Theory*, Vol.36, pp. 743–761.
- [3] Fanghella, P., Galletti, C., and Gianotti, E., 2006, “Parallel robots that change their group of motion,” *Advances in Robot Kinematics*, Springer, pp. 49–56.

- [4] Kiper, G., and Soylemez, E., 2011, “Modified Wren platforms”, *13th World Congress in Mechanism and Machine Science*, Guanajuato, Mexico, 19-25 June, 2011, IMD-123.
- [5] Kong, X., 2012, “Type synthesis of variable degree-of-freedom parallel manipulators with both planar and 3T1R operation modes,” *Proceedings of ASME 2012 International Design Engineering Technical Conferences & Computers and Information in Engineering Conference*, DETC2012-70621, August 12-15, 2012, Chicago, USA.
- [6] Zeng, Q, Ehmann, KF, and Cao, J, 2016, “Design of general kinematotropic mechanisms,” *Robotics and Computer-Integrated Manufacturing*, 38, pp. 67–81.
- [7] Kong, X. and Pfurner, M., 2015, “Type synthesis and reconfiguration analysis of a class of variable-DOF single-loop mechanisms,” *Mechanism and Machine Theory*, **85**, pp. 116–128.
- [8] Lopez-Custodio, P.C., Rico, J.M., Cervantes-Sánchez, J.J. and Perez-Soto, G.I., 2016, “Reconfigurable mechanisms from the intersection of surfaces,” *Journal of Mechanisms and Robotics*, 8(2), 021029.
- [9] Pfurner, M., and Kong, X., 2016, “Algebraic analysis of a new variable-DOF 7R mechanism”, In Philippe Wenger and Paul Flores, editors, *New Trends in Mechanism and Machine Science, Theory and Industrial Applications*, pp.71–79, Springer.
- [10] Zhang, K, and Dai, J.S., “Reconfiguration analysis of Wren platform and its kinematic variants based on reciprocal screw systems”. *Proceedings of the 14th IFToMM World Congress 2015 in Mechanism and Machine Science*, Paper Number OS8-022, October 25–30, 2015, Taipei, Taiwan.
- [11] Kong, X. 2017, “Standing on the shoulders of giants: A brief note from the perspective of kinematics,” *Chin J Mech Eng*, **30**(1): 1–2.
- [12] Kovalev, M.D., 1994, “Geometric theory of hinge mechanisms”, *Izvestiya RAN Seriya Matematicheskaya*, 58(1), pp. 45–70.
- [13] He, X., Kong, X., Chablat, D., Caro, S., and Hao, G., 2014, “Kinematic analysis of a single-loop reconfigurable 7R mechanism with multiple operation modes,” *Robotica*, Vol.32, pp. 1171–1188.

- [14] Feng, H., Chen, Y., Dai, J.S., Gogu, G., 2017, “Kinematic study of the general plane-symmetric Bricard linkage and its bifurcation variations,” *Mechanism and Machine Theory*, 116, pp. 89–104.
- [15] Husty, M.L. and Schröcker, H.-P., 2013, “Kinematics and algebraic geometry,” *In 21st Century Kinematics*, McCarthy, J.M. (ed), Springer, pp. 85–123.
- [16] Coste, M. and Demdah, K.M., 2015, “Extra modes of operation and self motions in manipulators designed for Schoenflies motion.” *Journal of Mechanisms and Robotics*, 7 (4), 041020.
- [17] Nurahmi, L., Caro, S., Wenger, P., Schadlbauer, J., and Husty, M., 2016, “Reconfiguration analysis of a 4-RUU parallel manipulator.” *Mechanism and Machine Theory*, 96, pp.269–289.
- [18] Kong, X., 2016, “Reconfiguration analysis of a variable degrees-of-freedom parallel manipulator with both 3-DOF planar and 4-DOF 3T1R operation modes,” Proceedings of the ASME 2016 International Design Engineering Technical Conferences & Computers and Information in Engineering Conference, DETC2016-59203, August 21–24, 2016, Charlotte, North Carolina, USA.
- [19] Arponen, T., Piipponen, S., and Tuomela, J., 2013, “Kinematical analysis of Wunderlich mechanism,” *Mechanism and Machine Theory*, **70**, pp. 16–31.
- [20] Müller, A. and Piipponen, S., 2015, “On regular kinematotropies,” *Proceedings of the 14th World Congress in Mechanism and Machine Science*, Paper Number OS2-046, October 25–30, 2015, Taipei, Taiwan.
- [21] Kuo, C.-H., Su, J.-W., 2017, “Configuration analysis of a class of reconfigurable cube mechanisms: Mobility and configuration isomorphism,” *Mechanism and Machine Theory*, **107**, pp. 369–383.
- [22] Lopez-Custodio, P.C., Rico, J.M., Cervantes-Sanchez, J.J., Perez-Soto, G.I., and Dez-Martnez, C.R., 2017. “Verification of the higher order kinematic analyses equations”, *European Journal of Mechanics A/Solids*, 61: pp. 198–215
- [23] Song, C.Y., Feng, H., Chen, Y., Chen, I.-M., Kang, R., 2015, “Reconfigurable mechanism generated from the network of Bennett linkages,” *Mechanism and Machine Theory*, **88**, pp. 49–62.

- [24] Kong, X., 2017, “Reconfiguration analysis of multi-mode single-loop spatial mechanisms using dual quaternions”, *ASME Journal of Mechanisms and Robotics*, **9**(5), 051002.
- [25] Yang, A.T., 1969, “Displacement analysis of spatial five-link mechanisms using  $(3 \times 3)$  matrices with dual-number elements,” *ASME Journal of Engineering for Industry*, Vol.91, pp. 152–157.
- [26] Gervasi, P., Karakusevic, V., and Zsombor-Murray, P.J., 1998, “An algorithm for solving the inverse kinematics of a 6R serial manipulator using dual quaternions and Grassmannians,” In *Advances in Robot Kinematics: Analysis and Control*, Jadran Lenarčič, M. L. Husty (eds), Springer, pp. 383–392.
- [27] Radavelli, L., Simoni, R., De Pieri, E., and Martins, D., 2012, “A comparative study of the kinematics of robots manipulators by Denavit-Hartenberg and dual quaternion,” *Mecánica Computacional, Multi-Body Systems* Vol.31, pp. 2833–2848.
- [28] Gan, D., Liao, Q., Wei, S., Dai, J.S., and Qiao, S., 2008, “Dual quaternion-based inverse kinematics of the general spatial 7R mechanism,” *Proceedings of the Institution of Mechanical Engineers, Part C: Journal of Mechanical Engineering Science*, Vol.22, pp. 1593–1598.
- [29] Li, Z., and Schicho, J., 2015, “A technique for deriving equational conditions on the Denavit-Hartenberg parameters of 6R linkages that are necessary for movability,” *Mechanism and Machine Theory*, Vol.94, pp. 1–8.
- [30] McCarthy, J.M., 2000, *Geometric Design of Linkages*, Springer-Verlag, New York.
- [31] Selig, J. M., 2005, *Geometric Fundamentals of Robotics*, Springer, New York.
- [32] Thomas, F., 2014, “Approaching dual quaternions from matrix algebra,” *IEEE Transactions on Robotics* Vol.30, pp. 1037–1048.
- [33] Dai, J.S., 2015, “Euler-Rodrigues formula variations, quaternion conjugation and intrinsic connections,” *Mechanism and Machine Theory*, **92**, pp. 144–152.
- [34] Morton, B., and Elgersma, M., 1996, “A new computational algorithm for 7R spatial mechanisms,” *Mechanism and Machine Theory*, **31**(1), pp. 23–43.
- [35] Liao, Q., Liang, C., and Zhang, Q., 1993, “Synthesizing spatial 7R mechanism with 16-assembly configurations,” *Mechanism and Machine Theory*, **28**(5), pp. 715–720.

- [36] Kong, X. and Huang, C., 2009, “Type synthesis of single-DOF single-loop mechanisms with two operation modes,” *Reconfigurable Mechanisms and Robots*, KC Edizioni, pp. 141–146.
- [37] Kong, X., 2014, “Type synthesis of single-Loop overconstrained 6R spatial mechanisms for circular translation”, *Journal of Mechanisms and Robotics*, 6(4): 041016–041016-8
- [38] Mavroidis, C. and Roth, B., 1995, “New and revised overconstrained mechanisms”, *ASME Journal of Mechanical Design*, 117(1), pp. 75–82.
- [39] Zhang, K. and Dai, J.S., 2016, “Geometric constraints and motion branch variations for reconfiguration of single-loop linkages with mobility one,” *Mechanism and Machine Theory*, **106**, pp. 16–29.